General treatment of the multimode Jahn–Teller effect: study of fullerene cations

Harry Ramanantoanina,[a] Matija Zlatar,[b] Pablo García-Fernández,[c] Claude Daul[a] and Maja Gruden-Pavlović*[ad]

A general model for the analysis of the Adiabatic Potential Energy Surfaces (APES) of the molecules that are subject to the multimode Jahn–Teller effect is presented. The method utilizes the information obtained by DFT calculations on a distorted stationary point on the APES. The essence of the model is to express the distortion along a model minimal energy path called Intrinsic Distortion Path (IDP), projecting the geometry of the system on the normal modes of the either high-symmetry (HS) or low symmetry (LS) nuclear configuration. This allows us to determine the significance of all of the involved normal modes along a relevant particular path of distortion, and the direct calculation of the vibronic coupling constants. The IDP analysis is illustrated by the discussion of the multimode $H \otimes (g + 2h)$ JT effect in fullerene cations (C_{60}^+) giving a deep insight into the origin and the mechanism of vibronic coupling in fullerene based molecules.

1 Introduction

The theory of vibronic coupling, coupling between electronic states and nuclear displacements, has a long history,[1] and presents a sole mechanism responsible for all structural distortions in molecules and solids. The importance of the Jahn–Teller (JT) effect[1–3] is very well recognized, and goes well beyond academic discussions. The JT effect is known to influence the high-T_C superconductivity,[4,5] ferroelectric phase transitions in perovskite crystals, large magneto-resistance in manganites,[6] superconductivity in fullerides,[7–10] and many other properties, putting the study of this interesting phenomenon in the spotlight of research in various fields.

Despite the great progress and development of various experimental techniques for studying the Jahn–Teller (JT) effect,[1,11] computational methods are necessary to understand the microscopic origin and to get deeper insight into the vibronic coupling effects.[12] There is no doubt that the results obtained using high-level *ab initio* calculations give accurate

a Department of Chemistry, University of Fribourg, Chemin du Musée 9, 1700 Fribourg, Switzerland. E-mail: claude.daul@unifr.ch; Fax: +41 26 300 9738; Tel: +41 26 300 8700
b Center for Chemistry IChTM, University of Belgrade, Njegoševa 12, 11000 Belgrade, Serbia. E-mail: matijaz@chem.bg.ac.rs; Tel: +381 11 333 6754
c Ciencias de la Tierra y Física de la Materia Condensada, Universidad de Cantabria, Santander, Spain. E-mail: garciapa@unican.es
d Faculty of Chemistry, University of Belgrade, Studentski tgr 12-16, 11000 Belgrade, Serbia. E-mail: gmaja@chem.bg.ac.rs; Tel: +381 11 333 6754

values and a good account of experimental observations.[13–16] However, it is computationally expensive to run those simulations on large molecules, and expertise in the field is required for the simulation. On the other hand, Density Functional Theory (DFT) can be applied routinely to medium-to-large-sized molecules, even though treatment of the degenerate states requires special caution.[17–20] Special approaches like the multi-determinantal-DFT (MD-DFT)[21,22] have been shown to be successful for the analysis of JT active molecules.[21–28]

The distortion from a high symmetry (HS) nuclear arrangement, due to the JT effect, towards a lower symmetry (LS) energy minimum conformation is a displacement on the $3N - 6$ potential energy surface. In the ideal case, the distortion corresponds to the movements of nuclei along one normal mode that belongs to a non-totally symmetric irreducible representation (irrep) of the HS point group of a molecule. Nevertheless, this is true only for simple molecules. In complex molecules, the JT distortion is a superposition of many different normal coordinates, and quantifying the role played by different normal modes in symmetry breaking processes is of great importance. In order to tackle the multimode problem, the Intrinsic Distortion Path (IDP) analysis, in which the distortion is represented as a superposition of all totally symmetric normal modes in the LS minimum energy conformation, has been recently proposed.[22,26,28] This is in contrast with the usual treatment of the Jahn–Teller effect, starting from the HS point of the Adiabatic Potential Energy Surface (APES).[1] However, as we will show, all the required information, to calculate the vibronic coupling coefficients is also contained in the LS structure,

at least to a good approximation. Within the harmonic approximation the potential energy surface has a simple analytical form, so with this model, it is possible to directly separate the contributions of the different normal modes to the JT distortion, their energy contributions to the JT stabilization energy (E_{JT}) along a relevant particular path of distortion and the forces at the HS point, giving further insight into the vibronic coupling.

This work will show that the IDP and the well-known *interaction mode*[1,29,30] approaches can be connected, resulting in the rigorous and general model for the analysis of the APES of the molecules disposed to the multimode Jahn–Teller effect. Herein, we report utilities of both MD-DFT and IDP methods in analysis of the JT distortion in fullerene cations, $C_{60}{}^{+}$, an example of the non-trivial multimode problem, in a simple, efficient and non-empirical way.

2 Methodology

2.1 Multideterminantal-DFT

The MD-DFT approach[21,22] is exhaustively explained elsewhere.[22] Here, we will just give a brief summary of the computational procedure. Our starting points are the geometries and energies of the HS and LS nuclear configurations. The electronic state of the HS configuration requires in many cases to be represented with more than one single determinant, depending on the point group of the HS conformation and the irreps that unequally occupied molecular orbitals belong to. In order to obtain it, we use the Average of Configuration (AOC) type of calculation, where the degenerate orbitals are equally populated, in order to retain the A_1 symmetry of the total electron density in the HS point group. This yields the geometry of the HS species (step 1). The second step includes single point calculation imposing the HS symmetry on the nuclear geometry (obtained in step 1) and LS on the electron density. This is achieved by introducing an adequate occupation scheme in the Kohn–Sham molecular orbitals, in the specific LS point group, chosen according to the epikernel principle.[31,32] The third step is straightforward – geometry optimization constraining the structure to the specific LS point group, with the proper occupancy of Kohn–Sham orbitals. These calculations yield different geometries and energies that correspond to a minimum and a transition state on the APES. The JT stabilization energy E_{JT} is the difference in energy obtained in steps 2 and 3 for the structures with the same electron distribution.

2.2 Analysis of the multimode JT effect

While *ab initio* calculations are excellent tools for accurately predicting the geometries and energies of the high and low-symmetry stationary points of the APES, the physical origin of these results can only be understood with the use of *models*. Whereas much work has been devoted to the understanding of systems with a single active JT mode like, for example, the tetragonal distortion occurring in a transition metal complex with octahedral symmetry when the electronic state is E_g, much less is known about the behaviour of systems with many active modes, *i.e.* the so-called multimode JT problem.

A possibility to describe the multimode problem is through the use of the *interaction* mode.[1,29,30] In this method a single effective coordinate is created by using a linear combination of all the JT-active modes of the high-symmetry configuration:

$$Q_{int} = \sum_i c_i^{int} Q_i^{HS} \tag{1}$$

where Q_i^{HS} are the JT modes of the high-symmetry configuration, while c_i^{int} are the coefficients used to describe the interaction mode. The value of each c_i^{int} depends explicitly on the model employed to describe the JT effect in the system. Usually[1,30,33] these coefficients are obtained using a JT matrix including only linear coupling and harmonic force constants (F_i and K_i, respectively)

$$c_i^{int} = \frac{1}{\sqrt{N_{int}}} \frac{F_i}{K_i} \tag{2}$$

where $1/\sqrt{N_{int}}$ appears due to the normalization. Obviously, N_{int} depends on every F_i and K_i.[1,30,33] No general expressions exist to treat cases including cubic anharmonicity, combined JT and pseudo Jahn–Teller (PJT) problems, *etc.* In most practical applications[33,34] the interaction mode coefficients are chosen so that they describe the straight-line path between the HS and LS geometries. It must be noted that an interaction mode described in this way requires the inclusion of non-JT active modes like, but not restricted to, breathing totally-symmetric ones. In this sense the computationally obtained interaction mode is quite different from its original formulation given by eqn (2).

Recently, a new approach to *analyse* the multimode problem, called Intrinsic Distortion Path (IDP), has been proposed.[22,28] In this case the reference point for the method is the LS configuration, not the HS one, and the energy surface is assumed to be quadratic in the LS vibrational modes, Q_i^{LS}:

$$E(Q_1^{LS}, Q_2^{LS}, ..., Q_n^{LS}) = \sum_i \frac{1}{2} K_i^{LS} [(Q_i^{LS}(X)]^2 \tag{3}$$

where $Q_i^{LS}(X)$ is any geometry on the APES expressed in terms of the LS modes. In the case of IDP all the n modes included in eqn (3) are those which are totally symmetric in the LS configuration, since the reaction path going from the HS to the LS configuration will always respect the symmetry of the least symmetrical configuration.[35] The IDP is precisely this reaction path starting from the first-principles HS geometry and ending in the LS minimum using the simplified energy surface, eqn (3), instead of the full *ab initio* energy surface. It is clear that this *model* minimum energy path will differ from the fully *ab initio* one only in the cases of strongly anharmonic surfaces, but in most practical cases the differences are found to be small. The importance of the method is that it allows analysing various quantities associated with the JT effect. For example, using eqn (3) the Jahn–Teller energy can be approximated by a sum to each mode:

$$E_{JT} \approx E_{JT}^{IDP} = \sum_i \frac{1}{2} K_i^{LS} [Q_i^{LS}(HS)]^2 \tag{4}$$

where $Q_i^{LS}(HS)$ is the high-symmetry geometry expressed in terms of the LS modes. The fact that in previous calculations for various organic and organo-metallic systems the difference between E_{JT} and E_{JT}^{IDP} was very small (usually smaller than 10%)[22,24,26,28] shows that approximation of the APES by a harmonic surface is a good one in most cases. The reason behind this good behaviour may lie in the fact that the LS vibrational modes differ from the HS ones precisely due to the anharmonicity of the APES.

The analytical expression of the JT energy, eqn (4), allows obtaining the total force at the HS point directly.[22,28] This force can be projected on either HS or LS normal modes, that we denote F_i^{HS} and F_i^{LS}. The physical meaning of the linear vibronic coupling constant is the force along that particular mode, which drives the nuclei towards the minimum.[1] Thus, from the above considerations, the linear vibronic constants, typically defined *via* HS normal modes, can be evaluated as F_i^{HS}. The two sets of forces, along either LS or HS normal modes, while clearly being different, are however connected:

$$\vec{F}^{LS} = \mathbf{J}\vec{F}^{HS} \tag{5}$$

where $\vec{F}^{LS}$ and $\vec{F}^{HS}$ are column vectors with magnitudes of corresponding forces as elements, and $\mathbf{J}$ is a $(3N - 6) \times (3N - 6)$ Dushinsky matrix,[36] an orthonormal matrix which correlates the HS and LS normal modes (columns of corresponding $(3N) \times (3N - 6)$ matrices $\mathbf{Q}$):

$$\mathbf{J} = (\mathbf{Q}^{LS})^{\mathrm{T}}\mathbf{Q}^{HS} \tag{6}$$

Squares of the elements of the correlation matrix, J_{ki}^2, have the values between 0 and 1, thus $100 \times J_{ki}^2$ simply gives a percentage contribution of $\vec{Q}_i^{HS}$ to the $\vec{Q}_k^{LS}$. These coefficients are often collected in the so-called overlap matrix.[37]

As it will be shown in the next section both the interaction mode and the IDP provide with similar results in the case of a truly multimode problem, like the case of the fullerene ions. However, both have advantages and disadvantages. The simpler concept of the interaction mode allows its application in many situations like PJT molecules, where the origin of the distortion involves the interaction with an excited state, or state crossings like the ones occurring in the *hidden* JTE.[38–40] Having in mind that IDP only models the APES of one electronic state around a single minimum of the surface, it is clear that it is not applicable to these problems not being able to account for vibronic anharmonicity,[41] appearing typically along the PJT effect and could lead to particularly erroneous results in systems with hidden JT. However, and as seen above, the IDP is more rigorous than the interaction mode approach when treating non-JT modes and provides important chemical information like an approximation to the minimum energy path, or the decomposition of the Jahn–Teller energy in a mode-per-mode basis without the requirement of a case-by-case model. In fact, and contrary to the interaction mode method, the contributions of each mode along the path are not fixed in IDP, allowing an analysis of the importance of each one depending on their distance to the HS configuration.

Finally we would like to remark that both the interaction mode and the IDP rely on reducing a many dimension surface to a single unidimensional cross-section and so, are badly prepared to treat dynamics since, many vibrational modes will be lost in the simplification and do not allow for branching of the energy surface. Moreover, IDP deals with a single minimum which fully prevents inter-well transitions, calculating the tunneling splitting, *etc.* so care must be taken when dealing with those problems.

2.3 Computational procedure

The MD-DFT calculations, Section 2.1, give the E_{JT} and the geometries of the HS and LS species. All the DFT calculations have been carried out using the Amsterdam Density Functional program package, ADF2009.01.[42–44] The local density approximation (LDA) characterized by the Vosko–Willk–Nusair (VWN)[45] parametrization has been used for the symmetry constrained geometry optimizations. In addition, gradient-corrections (GGA) for exchange (OPTX)[46] and correlation (PBE),[47] *i.e.* the OPBE functional,[48] as well as, hybrid B3LYP functional[49,50] have also been used. An all electron Triple-zeta Slater-type orbitals (STO) plus one polarization function (TZP) basis set has been used for carbon atoms. All calculations were spin-unrestricted. AOC structure in the I_h point group was optimized using a *z*-matrix. In this way, it was possible to confine the geometry to the I_h point group, without letting it to distort directly to one of the LS subgroups. In general, separation of the orbital and the geometrical symmetry, as used in the calculation of the energies of the HS nuclear configurations, can be done using the SYMROT subblock in the QUILD program, version 2009.01,[51] provided in the ADF2009.01 program package. Analytical harmonic frequencies[52,53] and normal modes at the LS stationary points were calculated.

The JT distortion, R_{JT}, length of the distortion vector between the HS and LS geometries, is expressed in terms of, either HS, or LS normal modes, Section 2.2:

$$\vec{R}_{JT} = \sum_i w_i^{LS}\vec{Q}_i^{LS} = \sum_i w_i^{HS}\vec{Q}_i^{HS} \tag{7}$$

where w_i represent the contribution of the displacements along the mass-weighted HS or the LS normal coordinate to the $\vec{R}_{JT}$, and the JT distortion of each normal mode, for herein studied C_{60}^+ is given simply as $r_{JT} = |w|/\sqrt{(12)}$. Energy contribution of the HS modes to the E_{JT} can be estimated as $E_i^{HS} = 1/2F_i^{HS}r_{JT}$.

Matlab scripts for the extraction of all the necessary data from ADF outputs, and for the calculations of all the mentioned quantities can be obtained from authors upon request.

3 Results and discussion

The ground state of of the neutral C_{60} molecule belongs to the totally symmetric, A_g, irrep of the I_h point group, with the highest occupied molecular orbital being the fivefold degenerate, h_u, and the lowest unoccupied molecular orbital triply degenerate, t_{1u}. Hence, the ground electronic state of C_{60}^+, ^2H_u,

is JT active. The analysis of the JT effect in C_{60}^+ by group theory is very interesting due to the high dimensionality of the irreps present in the parent I_h point group.[54] Many studies have been devoted to fully understand these distortions and properties arising from them.[3,30,54–59] It is noteworthy to mention that high interest in preparing hole-doped C_{60} compounds[60–63] is due to the remarkable characteristics expected[64–66] in these materials. Therefore, we have chosen C_{60}^+ to show the utilities of both MD-DFT and IDP approaches, and to compare it with the interaction mode approach.

The symmetry of the vibrations that can couple with the electronic ground state, linearly JT active modes, is determined from the symmetrized direct product, $[H_u \otimes H_u] = A_g \oplus G_g \oplus 2H_g$. Since a_g modes do not change the symmetry, the linearly JT active modes in C_{60}^+ form a basis of the G_g and H_g irreps in the I_h point group, leading to the $H \otimes (g + 2h)$ JT problem.[1,3] It is interesting that this direct product is not simply reducible, as it contains the irrep H twice.

The distortion may lead to the structures belonging to D_{5d}, D_{3d} and D_{2h} point groups.[1,3,54,55] It has been shown that the minima on the APES belong either to D_{5d} or D_{3d} point groups, depending on the particular values of the vibronic coupling constants (F_i) while the structures with D_{2h} symmetry are considered to be saddle points.[54] The distortion to the D_{5d} is driven by h_g modes described by one set of the linear vibronic coupling coefficients (F_{hg}^b), independently of the vibronic coupling of the g_g modes, as the latter do not become totally symmetric in the D_{5d} point group. The distortion to the D_{3d} is achieved by the h_g modes with a different set of vibronic coupling coefficients (F_{hg}^a) together with the g_g modes. The part of the correlation table for the descent in symmetry from the I_h point group to D_{5d}, D_{3d} and D_{2h} point groups, relevant for this work, is presented in Table 1.

The MD-DFT results for the distortions of C_{60}^+ to the three different epikernel sub-groups of the I_h point group, using different exchange–correlation functionals, are summarized in Table 2. The $^2A_{1u}$ conformation in the D_{5d} point group is the global minimum, confirmed by the absence of any imaginary frequency, with a stabilization energy of around 600 cm^{-1}, independently of the level of theory. This value is in a good agreement with reported values so far.[55,59] An overlap matrix between normal modes in I_h and D_{5d} nuclear configurations (a matrix with J_{ki}^2 as elements, Section 2.2) and their frequencies are presented in Table 3.

Table 2 The JT stabilization energy E_{JT} (cm^{-1}) and JT radius R_{JT} (Å) for different distortions (from I_h to: D_{5d}, D_{3d} and D_{2h}) of C_{60}^+ obtained by MD-DFT and IDP models with different exchange–correlation functionals (LDA, OPBE and B3LYP)

	Symmetry Electronic state	D_{5d} $^2A_{1u}$	D_{3d} $^2A_{1u}$	D_{2h} ^2A_u	D_{2h} $^2B_{1u}$
LDA	E_{JT} (MD-DFT)	599	215	254	434
	E_{JT} (IDP)	584	162	219	417
	R_{JT}	0.151	0.038	0.068	0.120
OPBE	E_{JT} (MD-DFT)	596	228	266	444
	E_{JT} (IDP)	600	170	232	418
	R_{JT}	0.156	0.039	0.068	0.122
B3LYP	E_{JT} (MD-DFT)	647	261	276	509
	E_{JT} (IDP)	758	199	283	511
	R_{JT}	0.165	0.041	0.073	0.128

There are two types of conformations belonging to the D_{2h} point group, as expected from the group theory:[54] the $^2B_{1u}$, $^2B_{2u}$ and $^2B_{3u}$, which are iso-energetic, with a single imaginary frequency (b_{1g}, b_{2g} and b_{3g} respectively); and the ^2A_u state, higher in energy, with two imaginary frequencies (b_{1g} and b_{2g}). The distortion pathway from I_h to D_{2h} symmetry removes completely the electronic degeneracy. However, in D_{5d} and D_{3d} point groups, two irreps remain degenerate. The doubly degenerate electronic states in these LS point groups may be a subject of further ($E \otimes e$) JT distortion leading to two geometries with C_{2h} symmetry. The MD-DFT calculation revealed that these C_{2h} structures are higher in energy than the global minimum. This differs from the case of C_{60}^-, where a stable geometry of C_{2h} symmetry is predicted.[67] The $^2A_{1u}$ electronic state of C_{60}^+ in the D_{3d} point group has four imaginary frequencies (e_g and e_g), in accordance with the prediction of Ceulemans and Fowler.[54]

The IDP analysis gives a further insight into the vibronic coupling in C_{60}^+. The potential energy profile for the distortion from the I_h cusp to the D_{5d} global minimum presented in Fig. 1(a) clearly distinguishes two different regions. In the first region, the energy is changing fast, and most of the E_{JT} is obtained after 40% of the path. In the second region the molecule has just relaxed towards the global minimum. The difference between the direct path obtained in the interaction mode way and the IDP path is clearly demonstrated in Fig. 1(a).

An analysis of the multimode JT distortion, Fig. 1(b), shows that the distortion starts with the hardest frequency anti-squashing modes, mainly C–C stretch modes (the h_g7 and h_g8 modes, Table 3), followed by dominant contribution of

Table 1 Summary of the group theory considerations for the JT distortions in C_{60}^+

Distortion	$\Gamma_{el}{}^a$	$\Gamma_{JT}{}^b$	n^c	Origin of the LS a_1 vibs^d
$I_h \rightarrow D_{5d}$	$H_u \rightarrow A_{1u} + E_{1u} + E_{2u}$	$H_g \rightarrow A_{1g} + E_{1g} + E_{2g}$ $G_g \rightarrow E_{1g} + E_{2g}$	10	$2a_g$, $8h_g$
$I_h \rightarrow D_{3d}$	$H_u \rightarrow A_{1u} + 2E_u$	$H_g \rightarrow A_{1g} + 2E_g$ $G_g \rightarrow A_{1g} + A_{2g} + E_g$	16	$2a_g$, $6g_g$, $8h_g$
$I_h \rightarrow D_{2h}$	$H_u \rightarrow 2A_u + B_{1u} + B_{2u} + B_{3u}$	$H_g \rightarrow 2A_g + B_{1g} + B_{2g} + B_{3g}$ $G_g \rightarrow A_g + B_{1g} + B_{2g} + B_{3g}$	24	$2a_g$, $6g_g$, $8h_g$

^{a} Γ_{el} is irrep of the electronic state. ^{b} Γ_{JT} is irrep of the JT active vibrations. ^{c} n is the number of the totally symmetrical vibrations in the LS point group. ^{d} One component of the degenerate set of vibrations in the HS becomes a_1 in the LS point group.

Table 3 Part of the overlap matrix between normal modes of C_{60}^+ in D_{5d} and I_h nuclear configurations. Frequencies ($\bar{\nu}$) are given in cm^{-1}

| I_h	D_{5d} $\bar{\nu}$	$a_{1g}1$ 263.39	$a_{1g}2$ 431.02	$a_{1g}3$ 502.32	$a_{1g}4$ 712.11	$a_{1g}5$ 787.09	$a_{1g}6$ 1130.46	$a_{1g}7$ 1282.14	$a_{1g}8$ 1468.92	$a_{1g}9$ 1524.32	$a_{1g}10$ 1609.65
a_g1	501.24	0.0000	0.0008	0.9990	0.0000	0.0001	0.0000	0.0000	0.0000	0.0000	0.0000
a_g2	1522.13	0.0000	0.0000	0.0000	0.0000	0.0000	0.0003	0.0015	0.0009	0.9905	0.0066
g_g1	494.06	0.0000	0.0000	0.0000	0.0000	0.0000	0.0000	0.0000	0.0000	0.0000	0.0000
g_g2	574.41	0.0000	0.0000	0.0000	0.0000	0.0000	0.0000	0.0000	0.0000	0.0000	0.0000
g_g3	773.91	0.0000	0.0000	0.0000	0.0000	0.0000	0.0000	0.0000	0.0000	0.0000	0.0000
g_g4	1122.90	0.0000	0.0000	0.0000	0.0000	0.0000	0.0000	0.0000	0.0000	0.0000	0.0000
g_g5	1333.95	0.0000	0.0000	0.0000	0.0000	0.0000	0.0000	0.0000	0.0000	0.0000	0.0000
g_g6	1532.00	0.0000	0.0000	0.0000	0.0000	0.0000	0.0000	0.0000	0.0000	0.0000	0.0000
h_g1	265.69	0.9999	0.0001	0.0000	0.0000	0.0000	0.0000	0.0000	0.0000	0.0000	0.0000
h_g2	438.10	0.0001	0.9987	0.0008	0.0003	0.0001	0.0000	0.0000	0.0000	0.0000	0.0000
h_g3	722.51	0.0000	0.0003	0.0000	0.9996	0.0000	0.0001	0.0000	0.0000	0.0000	0.0000
h_g4	793.10	0.0000	0.0001	0.0001	0.0000	0.9995	0.0000	0.0001	0.0001	0.0001	0.0000
h_g5	1128.40	0.0000	0.0000	0.0000	0.0001	0.0001	0.9982	0.0004	0.0008	0.0005	0.0000
h_g6	1285.33	0.0000	0.0000	0.0000	0.0000	0.0001	0.0006	0.9952	0.0028	0.0015	0.0000
h_g7	1466.84	0.0000	0.0000	0.0001	0.0000	0.0001	0.0007	0.0027	0.9956	0.0006	0.0000
h_g8	1601.39	0.0000	0.0000	0.0000	0.0000	0.0001	0.0000	0.0000	0.0000	0.0070	0.9931
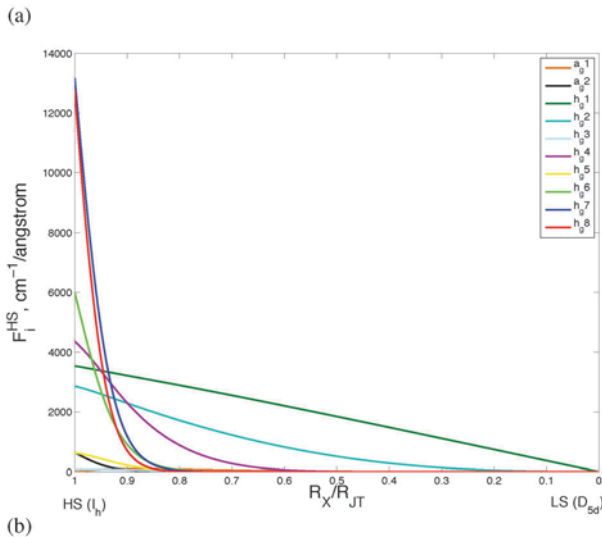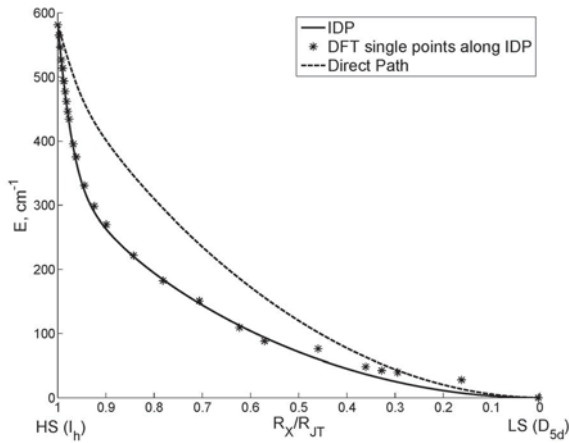
Fig. 1 Intrinsic Distortion Path Analysis of the $I_h \rightarrow D_{5d}$ multimode JT distortion in C_{60}^+: (a) change of the energy from I_h nuclear configuration to the D_{5d} global minimum; difference between the IDP path and the Direct path; (b) changes of the forces along the I_h normal modes.

contributions of the JT active modes, notably of the mode h_g1. As fullerenes are constructed out of five and six-member ring carbon atoms, it is interesting to note that in $C_6H_6^+$ and $C_5H_5^\bullet$, the distortion always starts with the hardest C–C stretch modes,[28] thus the IDP analysis may give a general trend in the distortion behaviour of the JT active molecule with the C–C bonds. In order to determine the linear vibronic coupling in C_{60}^+, we calculated the forces at the HS point concerning the distortion towards the D_{5d}, but also to the D_{3d} LS structures. These two distortion pathways are considered independently. The results are tabulated in Table 4. For the D_{3d} distortion, two forces (along h_g and g_g modes) are pushing the nuclei, but have the lower values than the forces for the D_{5d} distortion. The two hardest anti-squashing h_g modes have the largest

the lowest frequency squashing mode (the h_g1, Table 3). Similar distortion occurs in C_{60}^-,[67] except in the intensity of the

Table 4 Analysis of the multimode H ⊗ (g + 2h) JT effect in C_{60}^+ at the I_h nuclear configuration: the JT radii ($r_{JT,i}$, Å), square of the coefficients of the interaction mode (c_i^{int}), energy contributions (E_i^{HS}, cm^{-1}) and the forces (F_i^{HS}, 10^3 cm^{-1} $Å^{-1}$)[a] of the I_h normal modes (Q_i^{HS})

Q_i^{HS}	$I_h \rightarrow D_{5d}$[b] $r_{JT,i}$	$(c_i^{int})^2$	E_i^{HS}	F_i^{HS}	$I_h \rightarrow D_{3d}$[c] $r_{JT,i}$	$(c_i^{int})^2$	E_i^{HS}	F_i^{HS}
a_g1	0.0014	0.0001	0	0.013	0.0041	0.0116	1	0.332
a_g2	0.0009	0.0000	4	0.642	0.0006	0.0002	3	0.429
g_g1	0.0001	0.0000	0	0.015	0.0184	0.2367	16	1.503
g_g2	0.0001	0.0000	0	0.018	0.0016	0.0017	0	0.180
g_g3	0.0001	0.0000	0	0.015	0.0161	0.1818	27	3.398
g_g4	0.0001	0.0000	0	0.046	0.0092	0.0592	21	4.129
g_g5	0.0001	0.0000	0	0.087	0.0024	0.0040	2	1.435
g_g6	0.0002	0.0000	0	0.052	0.0069	0.0328	16	5.768
h_g1	0.1410	0.8760	246	3.542	0.0024	0.0039	0	0.084
h_g2	0.0429	0.0810	57	2.865	0.0149	0.1554	5	1.041
h_g3	0.0003	0.0000	0	0.083	0.0184	0.2360	30	3.347
h_g4	0.0201	0.0177	50	4.368	0.0007	0.0004	0	0.262
h_g5	0.0015	0.0001	2	0.633	0.0037	0.0096	2	1.683
h_g6	0.0096	0.0041	23	5.985	0.0042	0.0122	5	2.497
h_g7	0.0171	0.0129	117	13.177	0.0063	0.0278	14	4.815
h_g8	0.0135	0.0080	85	12.762	0.0062	0.0267	20	5.634
Total	0.1507[d]	1.0000	584	20.322[d]	0.0378[d]	1.0000	162	11.952[d]

[a] Linear vibronic coupling constants. [b] Distortion $I_h \rightarrow D_{5d}$ is driven by h_g^b and a_g modes and leads to the global minimum. [c] Distortion $I_h \rightarrow D_{3d}$ is driven by h_g^a, g_g and a_g modes. [d] Vector sum.

vibronic coupling coefficient, as it can be clearly seen from the IDP analysis, Fig. 1(b). Their contributions decrease rapidly along the path. Although, the squashing h_g1 mode has the smaller vibronic coupling coefficient, its contribution to the E_{JT} is the most important, Table 4, because it dominates along the whole distortion path, Fig. 1(b). Hence, to get the real physical picture of the JT effect, it is necessary to monitor the changes of the forces along the whole minimum energy path.

In order to make a comparison, we refer to the work of Manini et al.,[55] where coefficients are obtained in a way similar to the interaction mode approach, and are considered to be the benchmark results for this system.[56–58] Based on the DFT calculations, using the LDA functional, Manini et al.,[55] determined the linear vibronic interactions of all the JT active modes to the h_u HOMO of the neutral C_{60}. The calculated constants were used to predict the photo-emission spectrum of C_{60} and excellent agreement with experiment was found.[56] Contribution of the degenerate modes to the E_{JT} is overall in good agreement with values reported by Manini et al.,[55] Fig. 2. The only discrepancy refers to the contribution of the two totally symmetric normal modes to the distortion. Manini et al.,[55] have done their calculation from the neutral I_h C_{60} geometry as a starting point. However, in the IDP model we used the AOC geometry of C_{60}^+. The AOC occupancy of the the Kohn–Sham orbital is a restricted SCF computation to represent the partially filled shell. The nine electrons in the HOMO of C_{60}^+ are evenly distributed upon the ten spin orbitals (Section 2.1). Thus the neutral C_{60} and charged C_{60}^+ species obtained by AOC calculations have different geometries. Therefore, we obtained discrepancy in the vibronic coupling of totally symmetric normal modes. However, if we consider the neutral C_{60} as the HS point, we obtain the values for the energy contributions in agreement with Manini et al.,[55] Fig. 2, confirming the importance of the starting reference geometry.
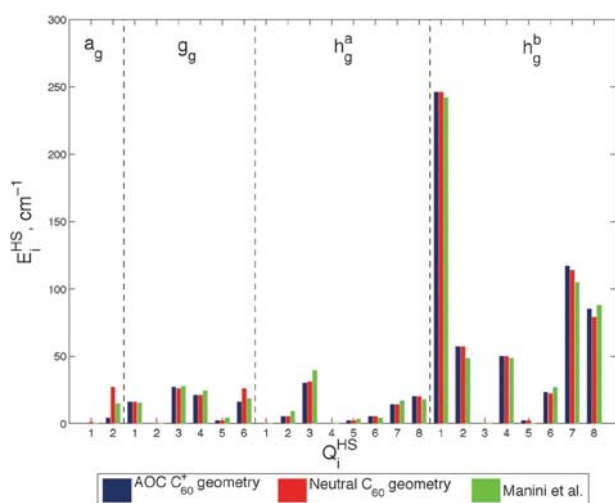

Fig. 2 Comparison of the energy contributions to the E_{JT} of different I_h normal modes in C_{60}^+ for different I_h geometries (from AOC geometry optimization of C_{60}^+ and from neutral C_{60}) with those from Manini et al.[55]

4 Conclusions

In this paper, a general approach to analyse the multimode JT distortion is presented and applied to study the APES in fullerene cations. The specific formulation of the JT distortion in terms of the Hessian of the LS minimum has several advantages. The LS structure is a true minimum on the APES, and the potential energy expression has a simple analytical form in the harmonic approximation. This allows us to obtain the approximated analytical expression for the force at the HS point, without any fitting, avoiding the problem of calculating energies and gradients around the HS cusp. It is shown that the IDP model and the well-known interaction mode approach can be connected easily, although LS structure is the reference point in the first one. Expressing the distortion along the minimal energy path from the HS to the LS minimum gives the change of contribution of different normal modes to the JT distortion, as well as to the E_{JT}. By means of all mentioned above, the static part of the multimode JT problem can be solved.

All the coupling coefficients were calculated for C_{60}^+, and the discrepancy with previously reported results has been explained. It was shown that one of the crucial points is the proper determination of the geometry of both HS and LS species. Taking the relevant neutral fullerene molecule as a reference HS point is an unnecessary approximation, since the ionization will affect the geometry, even if the geometry is constrained to the HS point group. Hence, the AOC calculation is the method of choice for analysing JT active species in the HS point group, even if the difference in geometry concerning analogue neutral molecules is not big. Inspection of the IDP in C_{60}^+ revealed that the stabilization of the energy is mostly achieved by the highest frequency anti-squashing h_g modes, relatively early along the IDP, while the relaxation of the geometry arrives in the final part of the IDP and encounters by the softer squashing h_g mode.

Quantifying the JT distortion in this simple and efficient way is of great interest not only for fullerene ions, but also for all JT active molecules because the experimental determination of the JT parameters is very difficult and depends on the model used. Since MD-DFT in conjunction with IDP is a fully non-empirical method, a fast and accurate, it can be considered as a reliable tool for better understanding of JT phenomena. Moreover, this approach is giving chemical insight into the origin and the mechanism of the vibronic coupling. Extension of the model for treatment of the PJT systems is currently under development in our groups.

Acknowledgements

References

1 I. B. Bersuker, *The Jahn-Teller Effect*, Cambridge University Press, Cambridge, 2006.

2 H. A. Jahn and E. Teller, *Proc. R. Soc. London, Ser. A*, 1937, **161**, 220–235.

3 C. C. Chancey and M. C. M. O'Brien, *The Jahn–Teller Effect in C_{60} and Other Icosahedral Complexes,* Princeton University Press, Princeton, 2006.

4 J. G. Bednorz and K. A. Müler, *Z. Phys. B: Condens. Matter*, 1986, **64**, 189–193.

5 J. G. Bednorz and K. A. Müler, in *Perovskite-type Oxides—The New Approach to High-Tc Superconductivity*, ed. G. Ekspang, World Scientific Publishing Co., Singapore, 1993, pp. 424–457.

6 A. J. Millis, *Nature*, 1998, **392**, 147–150.

7 O. Gunnarsson, *Nat. Mater.*, 2008, **7**, 176–177.

8 T. T. M. Palstra, *Nat. Mater.*, 2008, **7**, 350–351.

9 O. Gunnarsson, *Rev. Mod. Phys.*, 1997, **69**, 575–606.

10 O. Gunnarsson, J. E. Han, E. Koch and V. H. Crespi, *Superconductivity in Complex Systems*, in *Structure and Bonding*, ed. K. A. Müller and A. Bussmann-Holder, Springer, Berlin/Heidelberg, 2005, vol. 114, pp. 1352–1354.

11 V. V. GudkovandI. B. Bersuker,*Vibronic Interactions and Jahn–Teller effect: Theory and Applications*, in *Progress in Theoretical Chemistry and Physics*, ed. M. Atanasov, C. A. Daul and P. Tregenna-Piggott, Springer, Heidelberg, Dordrecht, London, New York, 2012, vol. 23, pp. 143–146.

12 H. J. Wörner and F. Merkt, *Angew. Chem., Int. Ed.*, 2009, **48**, 6404–6424.

13 M. J. Paterson, M. J. Bearpark, M. A. Robb, L. Blancafort and G. A. Worth, *Phys. Chem. Chem. Phys.*, 2005, **7**, 2100–2115.

14 P. H. Harbach and A. Dreuw, *Chem. Phys.*, 2010, **377**, 78–85.

15 P. Mondal, D. Opalka, L. V. Poluyanov and W. Domcke, *J. Chem. Phys.*, 2012, **136**, 084308.

16 P. Garcia-Fernandez, A. Trueba, M. T. Barriuso, J. A. Aramburu and M. Moreno, *Vibronic Interactions and Jahn–Teller effect: Theory and Applications*, in *Progress in Theoretical Chemistry and Physics*, ed. M. Atanasov, C. A. Daul and P. Tregenna-Piggott, Springer, Heidelberg, Dordrecht, London, New York, 2012, vol. 23, pp. 105–142.

17 I. B. Bersuker, *J. Comput. Chem.*, 1997, **18**, 260–267.

18 I. G. Kaplan, *J. Mol. Struct.*, 2007, **838**, 39–43.

19 M. Atanasov and C. Daul, *Chimia*, 2005, **59**, 504–510.

20 D. Reinen, M. Atanasov and W. Massa, *Z. Anorg. Allg. Chem.*, 2006, **632**, 1375–1398.

21 R. Bruyndonckx, C. Daul, P. T. Manoharan and E. Deiss, *Inorg. Chem.*, 1997, **36**, 4251–4256.

22 M. Zlatar, C.-W. Schläpfer and C. Daul, *The Jahn–Teller-Effect, Fundamentals and Implications for Physics and Chemistry*, in *Springer Series in Chemical Physics*, ed. H. Koeppel, D. R. Yarkoni and H. Barentzen, Springer, Heidelberg, Dordrecht, London, New York, 2009, vol. 97, pp. 131–165.

23 T. K. Kundu, R. Bruyndonckx, C. Daul and P. T. Manoharan, *Inorg. Chem.*, 1999, **38**, 3931–3934.

24 M. Gruden-Pavlović, M. Zlatar, C.-W. Schläpfer and C. Daul, *THEOCHEM*, 2010, **954**, 80–85.

25 M. Zlatar, M. Gruden-Pavlović, C.-W. Schläpfer and C. Daul, *Chimia*, 2010, **64**, 161–164.

26 M. Zlatar, M. Gruden-Pavlović, C.-W. Schläpfer and C. Daul, *THEOCHEM*, 2010, **954**, 86–93.

27 M. Zlatar, C.-W. Schläpfer, E. P. Fowe and C. Daul, *Pure Appl. Chem.*, 2009, **81**, 1397–1411.

28 M. Gruden-Pavlović, P. Garcia-Fernandez, L. Andjelković, C. Daul and M. Zlatar, *J. Phys. Chem. A*, 2011, **115**, 10801–10813.

29 I. B. Bersuker and V. Z. Polinger, *Vibronic interactions in Molecules and Crystals*, Springer-Verlag, Berlin, 1989.

30 V. Khlopin, V. Polinger and I. Bersuker, *Theor. Chim. Acta*, 1978, **48**, 87–101.

31 A. Ceulemans and L. G. Vanquickenborne, *Stereochemistry and Bonding*, in *Structure and Bonding*, Springer, Berlin/Heidelberg, 1989, vol. 71, pp. 125–159.

32 A. Ceulemans, D. Beyens and L. G. Vanquickenborne, *J. Am. Chem. Soc.*, 1984, **106**, 5824–5837.

33 Y. Liu, I. B. Bersuker, W. Zou and J. E. Boggs, *J. Chem. Theory Comput.*, 2009, **5**, 2679–2686.

34 M. Atanasov, D. Ganyushin, D. A. Pantazis, K. Sivalingam and F. Neese, *Inorg. Chem.*, 2011, **50**, 7460–7477.

35 R. G. Pearson, *Symmetry Rules for Chemical reactions*, A Willey-Interscience Publication, New York, 1976.

36 F. Duschinsky, *Acta Physicochim. URSS*, 1937, **7**, 551–566.

37 W. Hug and M. Fedorovsky, *Theor. Chem. Acc.*, 2008, **119**, 113–131.

38 P. Garcia-Fernandez, I. B. Bersuker and J. E. Boggs, *Phys. Rev. Lett.*, 2006, **96**, 163005.

39 I. B. Bersuker, *The Jahn–Teller-Effect Fundamentals and Implications for Physics and Chemistry*, in *Springer Series in Chemical Physics*, ed. H. Koeppel, D. R. Yarkoni and H. Barentzen, Springer, Heidelberg, Dordrecht, London, New York, 2009, vol. 97, pp. 3–23.

40 P. Garcia-Fernandez and I. B. Bersuker, *Phys. Rev. Lett.*, 2011, **106**, 246406.

41 I. B. Bersuker, *Electronic Structure and Properties of Transition Metal Compounds*, John Wiley and Sons, Hoboken, New Jersey, 2010.

42 E. J. Baerends, J. Autschbach, D. Bashford, A. Bérces, F. M. Bickelhaupt, C. Bo, P. M. Boerrigter, L. Cavallo, D. P. Chong, L. Deng, R. M. Dickson, D. E. Ellis, M. van Faassen, L. Fan, T. H. Fischer, C. F. Guerra, A. Ghysels, A. Giammona, S. van Gisbergen, A. Götz, J. Groeneveld, O. Gritsenko, M. Groening, F. Harris, P. van den Hoek, C. Jacob, H. Jacobsen, L. Jensen, G. van Kessel, F. Kootstra, M. V. Krykunov, E. van Lenthe, D. A. McCormack, A. Michalak, M. Mitoraj, J. Neugebauer, V. P. Nicu, L. Noodleman, V. P. Osinga, S. Patchkovskii, P. H. T. Philipsen, D. Post, C. C. Pye, W. Ravenek, J. I. Rodriguez, P. Ros, P. R. T. Schipper, G. Schreckenbach, M. Seth, J. G. Snijders, M. Sola, M. Swart, D. Swerhone, G. te Velde, P. Vernooijs, L. Versluis, L. Visscher, O. Visser, F. Wang, T. A. Wesolowski, E. M. van Wezenbeek, G. Wiesenekker, S. K. Wolff, T. K. Woo, A. L. Yakovlev and T. Ziegler, *ADF2009.01*, 2009, http://www.scm.com.

43 C. F. Guerra, J. G. Snijders, G. te Velde and E. J. Baerends, *Theor. Chem. Acc.*, 1998, **99**, 391–403.

44 G. te Velde, F. M. Bickelhaupt, S. J. A. van Gisbergen, C. F. Guerra, E. J. Baerends, J. G. Snijders and T. Ziegler, *J. Comput. Chem.*, 2001, **22**, 931–967.

45 S. Vosko, L. Wilk and M. Nusair, *Can. J. Phys.*, 1980, **58**, 1200–1211.

46 N. C. Handy and A. J. Cohen, *Mol. Phys.*, 2001, **99**, 403–412.

47 J. P. Perdew, K. Burke and M. Ernzerhof, *Phys. Rev. Lett.*, 1996, **77**, 3865–3868.

48 M. Swart, *J. Chem. Theory Comput.*, 2008, **4**, 2057–2066.

49 A. D. Becke, *J. Chem. Phys.*, 1993, **98**, 1372–1377.

50 P. Stephens, F. Devlin, C. Chabalowski and M. Frisch, *J. Phys. Chem.*, 1994, **98**, 11623–11623.

51 M. Swart and F. M. Bickelhaupt, *J. Comput. Chem.*, 2007, **29**, 724–734.

52 A. Bérces, R. M. Dickson, L. Fan, H. Jacobsen, D. Swerhone and T. Ziegler, *Comput. Phys. Commun.*, 1997, **100**, 247–262.

53 H. Jacobsen, A. Bérces, D. Swerhone and T. Ziegler, *Comput. Phys. Commun.*, 1997, **100**, 263–276.

54 A. Ceulemans and P. W. Fowler, *J. Chem. Phys.*, 1990, **93**, 1221–1234.

55 N. Manini, A. Dal Corso, M. Fabrizio and E. Tosatti, *Philos. Mag. B*, 2001, **81**, 793–812.

56 N. Manini, P. Gattari and E. Tosatti, *Phys. Rev. Lett.*, 2003, **91**, 196402.

57 N. Manini, *Phys. Rev. A*, 2005, **71**, 032503.

58 I. D. Hands, L. M. Sindi, J. L. Dunn and C. A. Bates, *Phys. Rev. B: Condens. Matter Mater. Phys.*, 2006, **74**, 115410.

59 M. Saito, *Phys. Rev. B: Condens. Matter Mater. Phys.*, 2002, **65**, 220508.

60 C. A. Reed and R. D. Bolskar, *Chem. Rev.*, 2000, **100**, 1075–1120.

61 C. A. Reed, K.-C. Kim, R. D. Bolskar and L. J. Mueller, *Science*, 2000, **289**, 101–104.

62 C. Bruno, I. Doubitski, M. Marcaccio, F. Paolucci, D. Paolucci and A. Zaopo, *J. Am. Chem. Soc.*, 2003, **125**, 15738–15739.

63 M. Ricco, D. Pontiroli, M. Mazzani, F. Gianferrari, M. Pagliari, A. Goffredi, M. Brunelli, G. Zandomeneghi, B. H. Meier and T. Shiroka, *J. Am. Chem. Soc.*, 2010, **132**, 2064–2068.

64 M. Granath and S. Östlund, *Phys. Rev. B: Condens. Matter Mater. Phys.*, 2002, **66**, 180501.

65 P. Paci, E. Cappelluti, C. Grimaldi, L. Pietronero and S. Strässler, *Phys. Rev. B: Condens. Matter Mater. Phys.*, 2004, **69**, 024507.

66 M. Lüders, N. Manini, P. Gattari and E. Tosatti, *Eur. Phys. J. B*, 2003, **35**, 57–68.

67 H. Ramanantoanina, M. Gruden-Pavlović, M. Zlatar and C. Daul, *Int. J. Quantum Chem.*, 2012, DOI: 10.1002/qua.24080.